A Study On The Governing Parameters Of MHD Mixed Convection Problem In A Ventilated Cavity Containing A Centered Square Block

M. U. Ahammad, M. M. Rahman, M. L. Rahman

Abstract: This paper reports the results of a numerical analysis of the influence of various parameters for the combined free and forced convection problem in a vented cavity with a centered heat generating element. Forced convection flow conditions are imposed by providing an inlet at the bottom of the left vertical wall and an outlet opening at the top of the opposite sidewall. Numerical solutions of the considered governing equations for the present study are obtained using the finite element method. The influence of Hartmann number, Prandtl number and Reynolds number on the flow and thermal fields is carried out and findings are presented by the streamlines and isotherms. Moreover, the heat transfer characteristic of the enclosure is displayed in terms of average Nusselt number and the dimensionless average bulk fluid temperature. Based on the computational results, it is noted that the studied parameters play a significant role on both the flow and thermal field.

Index Terms: Governing parameters, Hartmann number, Mixed convection, Prandtl number, Reynolds number, Ventilated cavity.

1 INTRODUCTION

A mixed convection flow and heat transfer of an electrically conducting fluid in a cavity in the presence of magnetic field often encounters in engineering circumstances. The applications include the cooling of electronic devices, furnaces, design of solar collectors, thermal design of building, air conditioning and drying technologies etc. The study of flow and heat transfer within obstructed enclosures are arisen frequently in many engineering applications to improve heat transfer such as micro-electronic device, flat-plate condensers in refrigerator etc. Following literature review shows that many researchers had considered mixed convection in enclosures with heated body. A numerical study for mixed convection in a square cavity due to heat generating rectangular body effect of cavity exit port locations was performed by Shuja *et al.* [1]. Rahman *et al* [2] presented the mixed convection flow problem in a rectangular ventilated cavity having a centered heat conducting square cylinder. Natural convection in a rectangular cavity with energy sources and electrically conducting fluid with sinusoidal temperature at the bottom wall was studied by Obayedullah *et al.* [3]. Papanicolaou and Jaluria [4] analyzed mixed convection from an isolated heat sources within a rectangular enclosure. Nasrin and Alim [5] have been carried out the effect of physical parameters on forced convection flow along a horizontal corrugated pipe with nanofluid. For the assisting forced flow patterns; Manca *et al.* [6] investigated experimentally mixed convection in a channel with an open cavity.

- *M. U. Ahammad is an assistant professor of mathematics in Dhaka University of Engineering and Technology (DUET),Gazipur-1700 and a Ph.D.fellow (Math) in Rajshahi University, Bangladesh, E-mail: main3737@gmail.com*
- *M. M. Rahman is a professor of mathematics in Bangladesh University of Engineering and Technology (BUET),Dhaka-1000, Bangladesh*
- *M. L. Rahman is a professor of mathematics in Rajshahi University, Rajshahi-6205, Bangladesh*

Two types of fluid motions such as parallel forced flow in the channel and the recirculation flow inside the cavity were found by the authors. Raji and Hasnaoui [7] studied the opposing mixed convection in a rectangular cavity heated from the side with a constant heat flux using the finite difference method. The problem of steady laminar forced convection inside a square cavity with inlet and outlet ports was presented by Saeidi and Khodadadi [8]. Sharif *et al.* [9] studied the assisting flow of MHD mixed convection inside a ventilated enclosure. Al-Rashed and Badruddin [10].investigated heat transfer in a porous cavity. Billah *et al.* [11] investigated a simulation of MHD combined free and forced convection heat transfer enhancement in a double lid-driven blocked enclosure. Kumar and Dalal [12] studied free convection around a heated square cylinder kept in an enclosure for the Reynolds number varied as 10^3 to 10^6 and reported that the uniform wall temperature heating is quantitatively different from the uniform wall heat flux heating. The mixed convection in a ventilated square cavity with a heat conducting horizontal solid circular cylinder was analyzed by Rahman *et al.* [13]. Chamkha [14] focused an unsteady laminar combined convection flow and heat transfer of an electrically conducting and heat generating or absorbing fluid considering the effect of a magnetic field in a vertical lid-driven cavity. Oztop *et al.* [15] investigated the fluid flow characteristics of combined convection in a lid-driven cavity containing a circular body where the cavity was heated at the left wall, cooled at the right wall and other two walls of the enclosure were insulated. A Hydromagnetic mixed convection problem in a double-lid driven cavity with a heat-generating block have been computed to observe the effect of Prandtl number by Rahman *et al.* [16]. Gau *et al*. [17] performed an experimental study on combined free and forced convection in a horizontal rectangular channel heated from a side. Mamun *et al.* [18] numerically studied mixed convection heat transfer in a bottom heated trapezoidal enclosure along with a moving upper wall and in this work the consequence of Richardson number, aspect ratio as well as rotational angle of the optimum trapezoidal cavity are presented by the authors. Hasanuzzaman *et al*. [19] analyzed the effects of variables on natural convective heat transfer through V-corrugated vertical plates. Mehmet and Elif [20] investigated natural convective flow in a rectangular enclosure having electrically conducting fluid with a magnetic field to find the inclination effect of the enclosure. Very recent an analysis of modeling and simulation of MHD convective heat transfer of channel flow having a cavity was carried out by Munshi *et al* [21] The present work concentrates on the effects of Hartmann number, Prandtl number and Reynolds number which may differ in the flow and heat transfer behaviors on mixed convection in a bottom heated square cavity containing a heat generating block.

2 Model Specification

The physical model under consideration and coordinates chosen are shown in Fig. 1, along with the important geometric parameters. The system consists of a square cavity with sides of length L which contains a centered heat generating solid block. The square block is of thermal conductivity k_s that produces uniform heat *q* per unit volume. A uniform magnetic field is imposed to the right vertical wall in the horizontal direction. The top, left and right side walls are assumed to be insulated whereas the bottom wall is kept at a uniform temperature of T_h. The inflow opening located on the bottom of the left wall and the outflow opening of the same size is placed at the top of the opposite vertical wall. It is assumed that the size of each port is equal to one tenth of the cavity length ($w = 0.1\,L$), the incoming flow is at a uniform

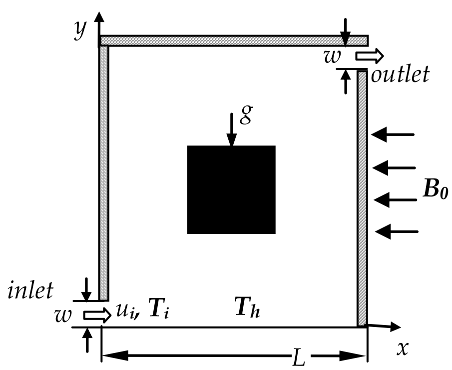

Fig. 1 Diagram for the present problem

velocity, u_i and at the ambient temperature, T_i. For all dependent variables the outgoing flow is supposed to have zero diffusion flux, i.e. convective boundary conditions (CBC). The rigid no-slip walls are considered for all solid boundaries.

3 Problem Formulation

The present flow is considered to be steady, two-dimensional, laminar and incompressible. The fluid properties are assumed to be constant and the Boussinesq's approximation is imposed to represent the buoyancy effect. Moreover, the viscous dissipation term in the energy equation is neglected. For the current work, the fluid flow and thermal fields within the cavity are governed by the Navier-Stokes and the energy equations. After non-dimensionalization, the governing equations may be written in the dimensionless form as follows:

Continuity Equation

$$\frac{\partial U}{\partial X}+\frac{\partial V}{\partial Y}=0 \qquad (1)$$

Momentum Equations

$$U\frac{\partial U}{\partial X}+V\frac{\partial U}{\partial Y}=-\frac{\partial P}{\partial X}+\frac{1}{\mathrm{Re}}\left(\frac{\partial^2 U}{\partial X^2}+\frac{\partial^2 U}{\partial Y^2}\right) \qquad (2)$$

$$U\frac{\partial V}{\partial X}+V\frac{\partial V}{\partial Y}=-\frac{\partial P}{\partial Y}+\frac{1}{\mathrm{Re}}\left(\frac{\partial^2 V}{\partial X^2}+\frac{\partial^2 V}{\partial Y^2}\right)+Ri\theta-\frac{Ha^2}{\mathrm{Re}}V \qquad (3)$$

Energy Equation

$$U\frac{\partial \theta}{\partial X}+V\frac{\partial \theta}{\partial Y}=\frac{1}{\mathrm{Re}\,\mathrm{Pr}}\left(\frac{\partial^2 \theta}{\partial X^2}+\frac{\partial^2 \theta}{\partial Y^2}\right) \qquad (4)$$

Energy Equation for solid block

$$\frac{K}{\mathrm{Re}\,\mathrm{Pr}}\left(\frac{\partial^2 \theta_s}{\partial X^2}+\frac{\partial^2 \theta_s}{\partial Y^2}\right)+Q=0 \qquad (5)$$

The dimensionless governing parameters in the preceding equations are the Reynolds number *Re*, Grashof number *Gr*, Prandtl number *Pr*, Richardson number *Ri*, Hartmann number *Ha*, heat generating parameter *Q* and solid fluid thermal conductivity ratio *K* which are defined respectively as

$$\mathrm{Re}=\frac{u_i L}{\upsilon}, Gr=\frac{g\beta\Delta T L^3}{\upsilon^2}, \mathrm{Pr}=\frac{\upsilon}{\alpha}, Ri=\frac{Gr}{\mathrm{Re}^2}, Ha^2=\frac{\sigma B_0^2 L^2}{\mu}, Q=\frac{qL^2}{k_s\Delta T}, K=\frac{k_s}{k}$$

where, $\alpha=\dfrac{k}{\rho c_p}$ indicates the thermal diffusivity of the fluid.

The associated dimensionless boundary conditions are stated as:

At the inlet $U=1, V=0, \theta=0$

At the outlet: Convective boundary condition (CBC), $P=0$

At the heated bottom wall: $\theta=1$

At the left, right and top walls: $U=0, V=0, \dfrac{\partial \theta}{\partial N}=0$

At the solid-fluid interfaces: $\left(\dfrac{\partial \theta}{\partial N}\right)_{fluid}=K\left(\dfrac{\partial \theta_s}{\partial N}\right)_{solid}$

The average Nusselt number *Nu* at the heated wall is given by

$$Nu_{av}=-\int_0^1\left(\frac{\partial \theta}{\partial Y}\right)dX$$

and the bulk average fluid temperature in the enclosure is defined as $\theta_{av}=\int \theta \dfrac{d\overline{V}}{\overline{V}}$ where $\overline{V}$ is the cavity volume.

4 Numerical Procedure

The numerical technique applied in this study is based on the Galerkin weighted residual method of finite element formulation. The continuum domain is discretized into finite element meshes, which are made of non-uniform triangular elements. The governing nonlinear mass, momentum and energy equations are transferred into a system of integral equations by using Galerkin weighted residual method. Gauss quadrature method executes the integration involving each term of these equations. Then boundary conditions are imposed and Newton's method is applied for transforming the nonlinear algebraic equations into linear algebraic equations. At last, these linear equations are solved by means of triangular factorization method.

Grid Independent Test

In order to avoid the complexity of the computational domain, at first grid refinement test is important for this study. Different types of grid such as: 14313 nodes, 1986 elements; 24388 nodes, 3536 elements; 42913 nodes, 6386 elements; 70329 nodes, 10711 elements and 83304 nodes, 12600 elements have been used for the grid refinement analysis. Table 1 shows that the variations among the results are very negligible. Based on the results from the table the grid with 42913 nodes and 6386 elements are selected throughout the simulation.

TABLE 1

Grid Sensitivity Check at Ri = 1.0, Ha = 10.0, Re = 100 and Pr = 0.71

Elements (Nodes)	*1986 (14313)*	*3536 (24388)*	*6386 (42913)*	*10711 (70329)*	**12600 (83304)**
Nu	4.0511	4.1501	4.1510	4.1512	4.1513
θ_{av}	0.1905	0.1901	0.1897	0.1837	0.1831
Time(s)	385.219	493.235	682.985	698.703	927.359

Grid Independent Test

To validate the numerical code of our problem, the present numerical scheme has been compared with the numerical results of Oztop *et al*. [15] for mixed convection problem in a lid-driven enclosure having a circular body. The cavity was heated at the left side, cooled at the right side whereas other two walls of the enclosure were kept adiabatic. The comparison of the average Nusselt number at the hot wall between the present computation and those of the mentioned reference is shown in Table 2 that reveals very fine agreement with a greatest difference of 0.9%. These validations make an assertion of the current numerical code.

TABLE 2

Assessment of average Nusselt number at the hot wall of the cavity for Re = 1000, $Gr = 10^5$, C (x = 0.5, y = 0.5) between the present data and that of the Oztop *et al*. [15]

Present	*Oztop et al. [15]*	**Error (%)**
9.125	9.13	0.05
10.38	10.37	0.10
11.20	11.10	0.90

5 Results And Discussion

The effects of Hartmann number, Prandtl number and Reynolds number for a MHD mixed convection problem in a ventilated square cavity containing a heat generating block have been investigated. The results of the present study are explained in the forms of streamlines and isotherms. In addition, the heat transfer effects inside the enclosure are shown in terms of average Nusselt number Nu_{av} and the average fluid temperature θ_{av}

Effect of Hartmann Number

The streamlines and isotherms have been analyzed to explain the flow and thermal field structure of the mixed convection problem for different values of Hartmann number. The Prandtl number Pr, Reynolds number Re are chosen 0.71 and 100 respectively while the Hartmann number is varied from 0 to 100 for each of the three convective regimes of Ri=0.1, 1, 10. Fig. 2 shows the influence of Hartmann number on fluid flow and temperature distribution for the dominant forced convection, Ri = 0.1. The streamlines corresponding to different Hartmann number are shown in the left column of Fig. 2. In the absence of magnetic field (Ha = 0) the fluid flow is characterized by the open lines that squeezes above the inlet openings. It is also noted that a small anti-clockwise rotating vortex is developed at top just entrance of the cavity. For Ha = 20, the shape of the streamlines are found to be slight different and the circulating cell vanishes. Again in the case of the higher values of Ha (= 50 and 100), the streamlines are about identical and it is observed that these are almost horizontal and vertical of the cavity walls in the whole domain. The right column of figure 2 displays the corresponding isotherms for the aforementioned Hartmann numbers. For Ha = 0, the isothermal lines are crowded at the inlet and a thermal boundary layer is followed in the vicinity of the bottom hot wall of the cavity. Also a round shaped heat line appears surrounded the square block. The non-linearity of the temperature distribution increases with the mounting values of Hartmann number. In the case of higher magnetic field parameter it is found that high isotherms are concentrated near the heat generating block and for Ha = 100, the circular isotherm confines the centered block. When natural and forced convection are equally dominant, namely, Ri = 1, the effect of Hartmann number on streamlines and thermal fields are demonstrated in Fig 3. The mainstreams shrink from the left and top side and consequently the CCW vortex increases much and it spreads up to the top cavity wall while Ha = 0. For Ha = 20 it is seen that the open lines swell up over the whole cavity and a small eddy is found above the inlet. No vortex forms for larger values of Hartmann number and the streamlines become more vertical for Ha = 100. This is

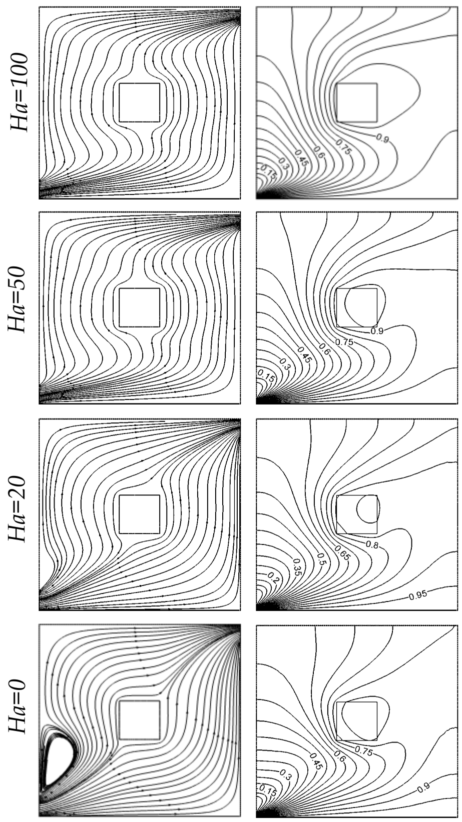

Fig. 2: Streamlines and isotherms for different values of *Ha*, at *Ri* = 0.1

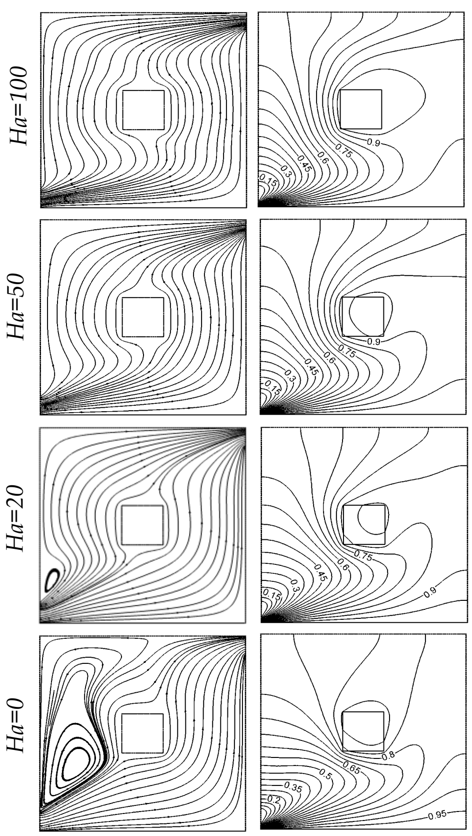

Fig. 3: Streamlines and isotherms for different values of *Ha*, at *Ri* = 1

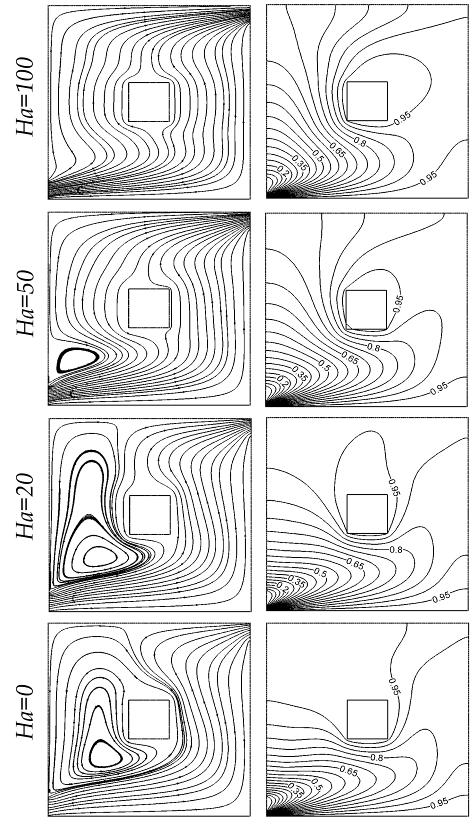

Fig. 4: Streamlines and isotherms for different values of *Ha*, at *Ri* = 10

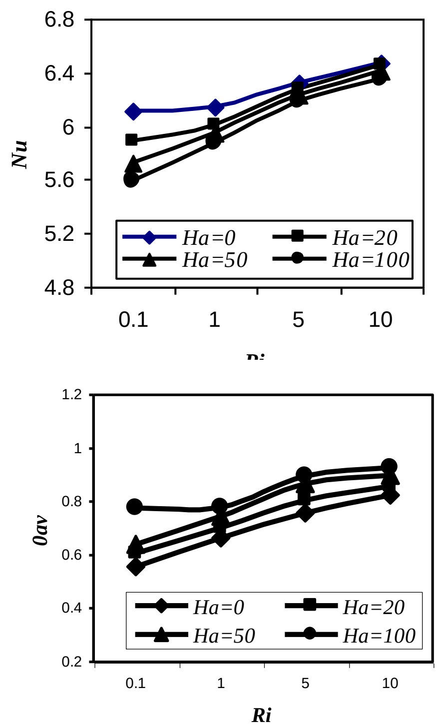

Fig. 5: Effect of different Hartmann number on average Nusselt number and average fluid temperature in the cavity while *Re* = 100, *Pr* = 0.71 and 0.1≤ *Ri*≤10.

Because most of the heat transfer process is carried out by conduction. In the case of lowest magnetic field the isotherms pattern changes above the heat generating block. But no significant change is found for growing magnetic field parameter comparatively with those of the case at *Ri* = 0.1. For the convective regime *Ri* = 10, Fig. 4 depicts the fluid flow characteristics and the temperature distributions for the variation of magnetic field parameter. For *Ha* = 0, it is seen that the core vortex expands more towards the right of the cavity and occupies the block indicating the enhancement of the flow strength of the vortex. As *Ha* increases the flow strength of the vortices reduces rapidly, major flows swell up and accordingly the vortex disappears while *Ha* = 100. From the right side of Fig. 4 it is noticed that at *Ha* = 0 the heat lines are packed below the block. The non-linearity of isotherms increases and the heat generating block is curbed by the topmost isothermal line for the cases of growing *Ha*. From Fig. 5 it is seen that as the magnetic field *Ha* decreases average Nusselt number *Nu* increases for all values of *Ri*. Thus higher *Nu* that is maximum heat transfer is found in the absence of magnetic field. Moreover for the increasing value of *Ri*, *Nu* increases for each of the four chosen values of *Ha* which is expected because of the supremacy of natural convection. In addition average fluid temperature is shown in Fig. 5 and from this figure it can be concluded that θ_{av} is about uniformly increase for the values of *Ha* = 20, 50, 100. But for *Ha* = 0, average temperature is identical in the region 0.1≤ *Ri*≤ 1 and it increases in the dominant natural convection domain. It is also observed that average temperature is lowest for *Ha* = 0.

Effect of Prandtl Number

The influence of Prandtl number on streamlines and isotherms are presented for fluid flow within a vented cavity of the mixed convection problem having a heat source. The Hartmann number *Ha*, Reynolds number *Re* are chosen 10 and 100 respectively while the Prandtl number is in the range 0.071 ≤ *Pr* ≤ 7.1 for each of the three convective regimes of *Ri*=0.1, 1, 10. The effect of *Pr* at the three different values of *Ri* on streamlines as well as isotherms are displayed in Figs. 6-8. From the left column of Fig. 6, it is seen that at *Ri* = 0.1, a small recirculation cell is formed near the left top corner of the inlet in the cavity while *Pr* = 0.071. This indicates that the fluid flow of the enclosure has been affected by the inertia force. There is no significant change in flow patterns for the rest three higher values of *Pr* at the dominant forced convection region, whereas it is observed that for the mixed convection and the dominant natural convection region the flow structure is influenced by varying *Pr* as shown in Fig. 7 and Fig. 8. As the buoyancy force increases with increasing *Ri*; the rotating cell becomes larger for a fixed value of *Pr* and higher values of *Ri.* The right column of Figs. 6-8 depicts the isotherms for the four considered values of *Pr*. These figures illustrate that at *Ri* = 0.1 and *Ri* = 1 with *Pr* = 0.071 the heat lines become thinner and highest isotherm line pass through the heat generating block but at the dominant free convection region the isothermal line move out from the obstacle. For all convective regimes with higher vales of *Pr* (= 1, 3, 7.1) it is seen that the isotherms become denser and top right cornered plume shape isotherms above the heated body are created. Also the higher Prandtl number gives more compact isotherms in the vicinity of the heat source. The average Nusselt number *Nu* and average fluid temperature θ_{av} in the studied cavity for different Prandtl numbers along with Richardson numbers has been focused in Fig. 9. It is noted that *Nu* increases with the rising value of *Pr* and accordingly optimum *Nu* is recorded for *Pr* = 7.1, due to the capability of the fluid with the highest Prandtl number is to carry more heat away from the heat generating block and dissipated through the outlet in the cavity. Besides this it can be followed that as θ_{av} decreases while *Pr* increases, minimum average temperature is found for large Prandtl number *Pr* = 7.1.

Effect of Reynolds Number

The streamlines and isotherms for the different values of *Re* with *Ha* = 10 and *Pr* = 0.71 have been presented in the Figs. 10-12. The left column of Fig. 10 shows the streamlines for the Reynolds number varied as 50 ≤ *Re* ≤ 500, whereas the dominant forced convection effect (*Ri* = 0.1) is considered. For the lower value of *Re* = 50 it is noticed that the fluid flow absorbs the whole cavity, diverges close to the heat source and the open lines are symmetric about diagonally. As the inertia force grows up with increasing *Re,* a CCW vortex is created above the inflow openings at *Re* = 200. This vortex expands sharply confining the heated block and another small clockwise vortex is found near the bottom right side of the cavity for the two higher values of *Re* (= 350, 500). This happened because the role of forced convection in the cavity becomes more significant with increasing *Re*. From the left column of Figs. 11 and 12 it can be highlighted that a noteworthy variation in flow behavior is found for the other two convective regimes of *Ri* (= 1, 10) with any particular Reynolds number. The corresponding effect of Reynolds number *Re* on the thermal field is exposed in the right column of Figs. 10-12. For *Re* = 50 and all *Ri* (= 0.1, 1, 10) it is apparent that the isotherms move out of the centered heat generating obstacle. For the considered three different convective regimes a thermal boundary layer is formed in the neighborhood of the bottom heated wall of the cavity and high isothermal lines are crowded at the lower part of the heat generating obstacle. Moreover, plume shape isotherms are viewed at the left side of the block for *Re* = 350 and *Re* = 500 at *Ri* = 0.1 while these are found at the top of the block for *Re* = 200 with *Ri* = 0.1 as well as *Re* (= 200, 350, 500) at the rest two regimes of *Ri*. It is also seen that thermal boundary-layer thickness increases as *Re* gets higher and the isothermal lines become denser at the adjacent area of the heated block in the mixed convection and natural convection dominated regions. Fig. 13 describes the effect of Reynolds number on average Nusselt number *Nu* and average fluid temperature θ_{av} in the cavity as a function of Richardson number. One can observes that the value of average Nusselt number increases as *Ri* increases for higher values of *Re* (=200, 350 and 500) whereas for *Re* = 50, *Nu* is almost constant for all *Ri*. Thus the greatest

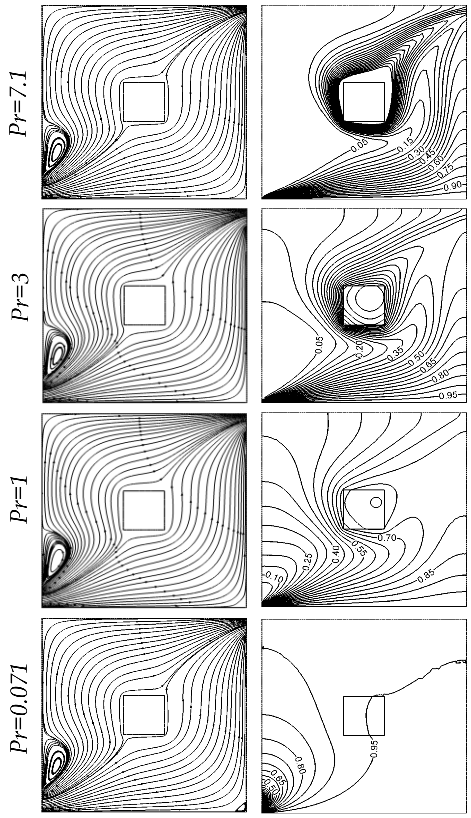

Fig. 6: Streamlines and isotherms for different values of *Pr*, at *Ri* = 0.1

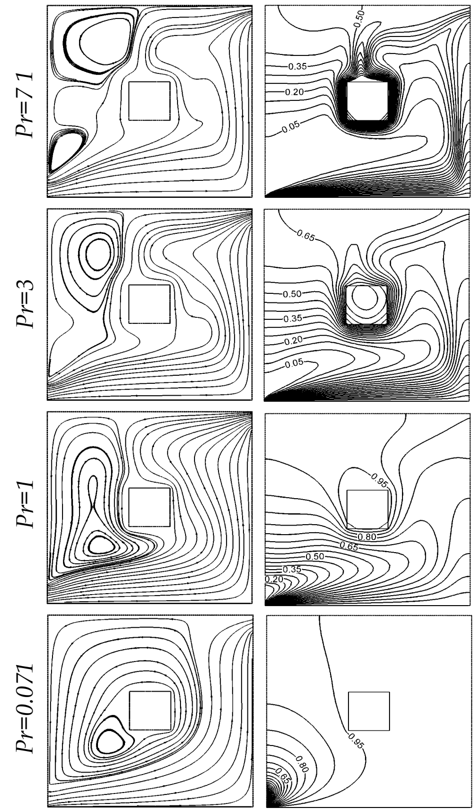

Fig. 8: Streamlines and isotherms for different values of *Pr*, at *Ri* = 10

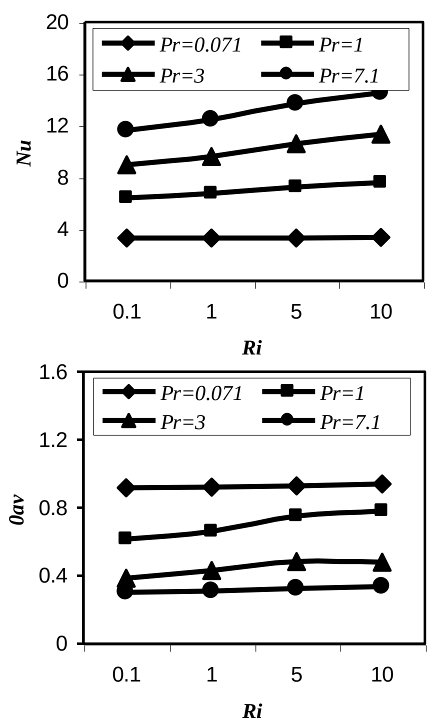

Fig. 9: Effect of different Prandtl number on average Nusselt number and average fluid temperature in the cavity while *Re* = 100, *Ha* = 10 and 0.1≤ *Ri*≤10.

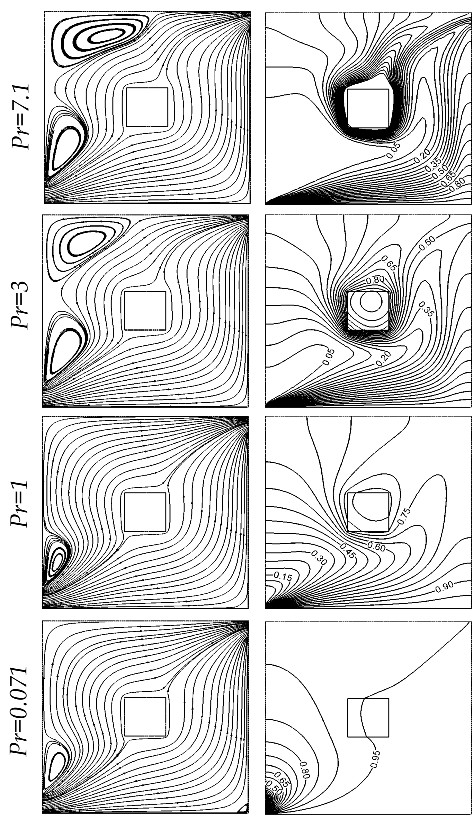

Fig. 7: Streamlines and isotherms for different values of *Pr*, at *Ri* = 1

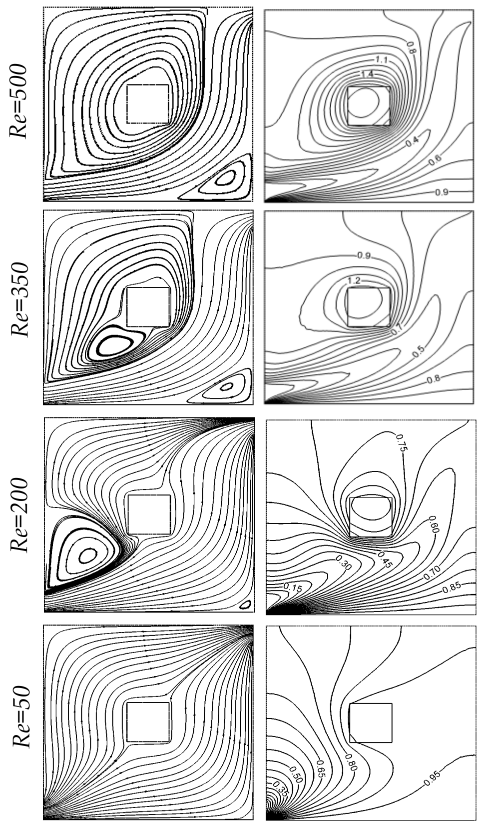

Fig. 10: Streamlines and isotherms for different values of *Re*, at *Ri* = 0.1

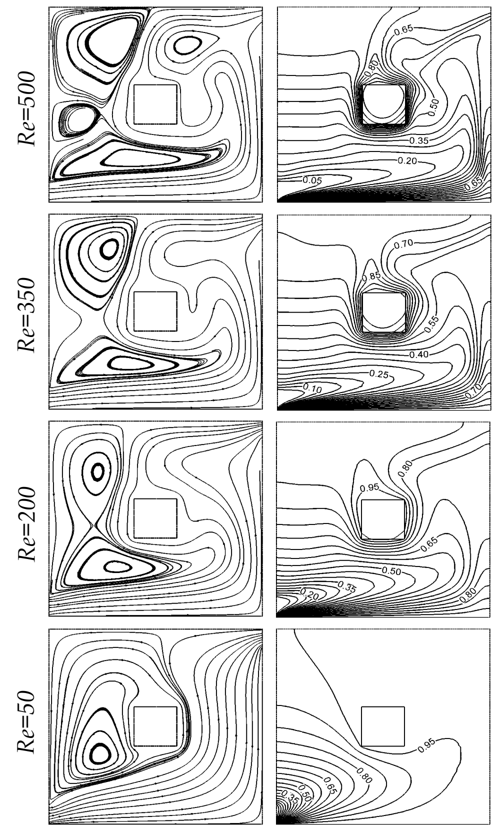

Fig. 12: Streamlines and isotherms for different values of *Re*, at *Ri* = 10

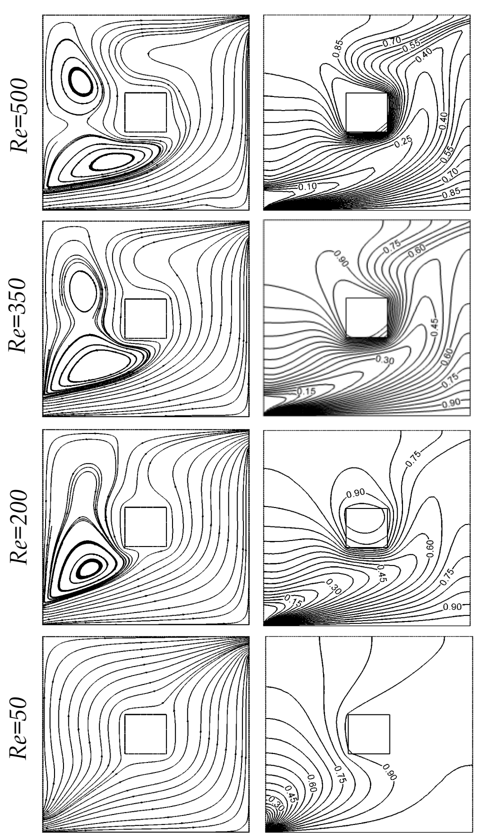

Fig. 11: Streamlines and isotherms for different values of *Re*, at *Ri* = 1

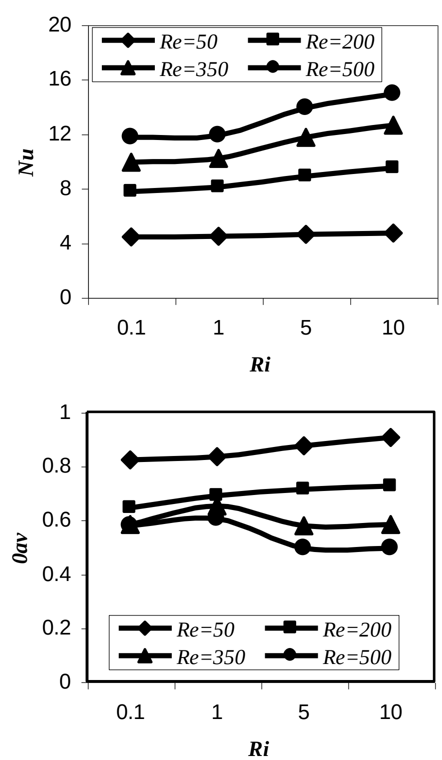

Fig. 13: Effect of different Reynolds number on average Nusselt number and average fluid temperature in the cavity while *Ha* = 10, *Pr* = 0.71 and 0.1≤ *Ri*≤10.

Heat transfer rate is found for the highest value of *Re*. On the other hand, the average fluid temperature in the cavity increases smoothly with increasing *Ri* for the lower values of *Re* (=50, 200). But for upper *Re* (= 350 and 500) it is noticed that θ_{av} increases as *Ri* varies from 0.1 to 1, decreases in the region 1 ≤ *Ri* ≤ 5 and θ_{av} is about independent beyond these regions. In addition lowest average fluid temperature occurs for the largest Reynolds number.

6. Conclusions

The present analysis addresses a problem on mixed convection two-dimensional laminar flow in a ventilated square enclosure with the variation of governing parameters such as Hartmann number (0 ≤ *Ha* ≤ 100), Prandtl number (0.071 ≤ *Pr* ≤ 7.1), Reynolds numbers (50 ≤ *Re* ≤ 500) and Richardson numbers (0.1 ≤ *Ri* ≤ 10). Detailed computations for the distribution of streamlines, isotherms, average Nusselt number at the heated wall and average fluid temperature in the cavity were performed to explore the effect of the mentioned parameters. In view of the obtained results, the following conclusions may be summarized**.** The flow field and temperature distribution are affected from the magnetic field. The decreasing of Hartmann number *Ha* increases the average Nusselt number but decreases the average fluid temperature in the cavity. The effects of Prandtl number *Pr* on streamlines are insignificant in the forced convection dominated region but significant in other two convective regimes. On the other hand, in all convective regimes the temperature distributions in the cavity are influenced much by Prandtl number. The average Nusselt number becomes higher and average temperature in the cavity becomes lower for the larger values of *Pr.* The Reynolds number *Re* always plays a crucial role on both flow and thermal fields. The highest value of *Re* gives the ceiling average Nusselt number and minimum average temperature in the cavity.

References

[1]. S.Z. Shuja, B.S. Yilbas, and M.O. Iqbal, "Mixed Convection in a Square Cavity Due to Heat Generating Rectangular Body Effect of Cavity Exit Port Locations," Int. J. of Numerical Methods for Heat and Fluid flow, vol. 10, no. 8, pp. 824-841, 2000.

[2]. M.M. Rahman, M. Elias, and M.A. Alim, "Mixed Convection Flow in a Rectangular Ventilated Cavity with a Heat Conducting Square Cylinder at the Center," J. of Engineering and Applied Sciences, vol. 4, no. 5, pp. 20-29, 2009.

[3]. M. Obayedullah, M.M.K. Chowdhury, and M.M. Rahman, "Natural Convection in a Rectangular Cavity Having Internal Energy Sources and Electrically Conducting Fluid with Sinusoidal Temperature at the Bottom Wall," International Journal of Mechanical and Materials Engineering, vol. 8, no. 1, pp. 73-78, 2013.

[4]. E. Papanicolaou, Y. Jaluria, "Mixed Convection from an Isolated Heat Source in a Rectangular Enclosure", Num. Heat Transfer, Part A, vol. 18, pp. 427-461, 1990.

[5]. R. Nasrin, M.A. Alim, "Analysis of Physical Parameters on Forced Convection Along a Horizontal Corrugated Pipe with Nanofluid", Engineering e-Transaction, vol. 7, no. 1, pp. 14-22, 2012.

[6]. O. Manca, S. Nardini, K. Vafai, "Experimental Investigation of Mixed Convection in a Channel with an Open Cavity," Numerical Heat Transfer, Part A, vol. 19, pp. 53-68, 2006.

[7]. A. Raji, M. Hasnaoui, "Mixed Convection Heat Transfer in a Rectangular Cavity Ventilated and Heated from the Side," Numer. Heat Transfer, Part A, vol. 33, pp. 533-548, 1998.

[8]. S.M. Saeidi, J.M. Khodadadi, "Forced Convection in a Square Cavity with Inlet and Outlet Ports," Int. J. of Heat and Mass Transfer, vol. 49, pp. 1896-1906, 2006.

[9]. U.M. Sharif, M.M. Rahman, M.A. Saklayen, M.M. Billah, M. Elias, "A Numerical Study of Assisting MHD Mixed Convection Inside a Ventilated Cavity," Engineering e-Transaction, vol. 7, no. 1, pp. 6-13, 2012.

[10]. A. Al-Rashed, and I.A. Badruddin, "Heat Transfer in a Porous Cavity," International Journal of Mechanical and Materials Engineering vol. 7, no. 1, pp. 1-8, 2012.

[11]. M.M. Billah, M.M. Rahman, R. Saidur, M. Hasanuzzaman, "Simulation of MHD Mixed Convection Heat Transfer Enhancement in a Double Lid-Driven Obstructed Enclosure," International Journal of Mechanical and Materials Engineering, vol. 6, no. 1, pp. 18-30, 2011.

[12]. A. Kumar De, and A. Dalal, "A Numerical Study of Natural Convection Around a Square Horizontal Heated Cylinder Placed in an Enclosure," International journal Heat Mass Transfer, vol. 49, pp. 4608-4623, 2006.

[13]. M.M. Rahman, M.A. Alim, S. Saha, and M.K. Chowdhury, "Mixed Convection in a Vented Square Cavity with a Heat Conducting Horizontal Solid Circular Cylinder," Journal of Naval Architecture and Marine Engineering, vol. 5, no. 2, pp. 37-46, 2008.

[14]. A.J. Chamkha, "Hydro Magnetic Combined Convection Flow in a Vertical Lid-Driven Cavity with Internal Heat Generation or Absorption," Numer. Heat Transfer Part A, vol. 41, pp. 529-546, 2002.

[15]. H.F. Oztop, Z. Zhao, and B. Yu, "Fluid Flow Due to Combined Convection in Lid-Driven Enclosure Having a Circular Body," Int. J. Heat and Fluid Flow, vol. 30, pp. 886-901, 2009.

[16]. M.M, Rahman, R. Nasrin, M.M. Billah, "Effect of Prandtl Number on Hydromagnetic Mixed Convection in a Double-Lid Driven Cavity with a Heat-Generating Obstacle," Engineering e-Transaction, vol. 5, no. 2, pp. 90-96, 2010.

[17]. C. Gau, Y.C. Jeng, C.G. Liu, “An Experimental Study on Mixed Convection in a Horizontal Rectangular Channel Heated From a Side,” ASME J. Heat Transfer, vol. 122, pp. 701-707, 2000.

[18]. M.A.H. Mamun, T.R. Tanim, M.M. Rahman, R. Saidur, and S. Nagata, “Mixed Convection Analysis in Trapezoidal Cavity with a Moving Lid,” International Journal of Mechanical and Materials Engineering, vol. 5, no. 1, pp. 18-28, 2010.

[19]. M. Hasanuzzaman, R. Saidur, M. Ali, H.H. Masjuki, “Effects of Variables on Natural Convective Heat Transfer Through V-Corrugated Vertical Plates,” International Journal of Mechanical and Materials Engineering, vol. 2, no.2, pp. 109-117, 2007.

[20]. C.E. Mehmet, and B. Elif, “Natural Convection Flow Under a Magnetic Field in an Inclined Rectangular Enclosure Heated and Cooled on Adjacent Walls,” Fluid Dynamics Research, vol. 38, pp. 564-590, 2006.

[21]. M.J.H. Munshi, A.K. Azad, R.A. Begum, M.B. Uddin, and M.M. Rahman, “Modeling and Simulation of MHD Convective Heat Transfer of Channel Flow Having a Cavity,” International Journal of Mechanical and Materials Engineering, vol. 8, no. 1, pp. 63-72, 2013.

[22]. Reddy, J.N. “An Introduction to Finite Element Analysis,” McGraw-Hill, New-York, 1993.